2-9-2011

Nonuniform high-gamma (60-500 Hz) power changes dissociate cognitive task and anatomy in human cortex

Charles M. Gaona

Mohit Sharma

Zachary V. Freudenburg

Jonathan D. Breshears

David T. Bundy

See next page for additional authors

Authors

Charles M. Gaona, Mohit Sharma, Zachary V. Freudenburg, Jonathan D. Breshears, David T. Bundy, Jarod Roland, Dennis L. Barbour, Gerwin Schalk, and Eric C. Leuthardt

Behavioral/Systems/Cognitive

Nonuniform High-Gamma (60–500 Hz) Power Changes Dissociate Cognitive Task and Anatomy in Human Cortex

Charles M. Gaona,[1] Mohit Sharma,[1] Zachary V. Freudenburg,[3] Jonathan D. Breshears,[2] David T. Bundy,[1] Jarod Roland,[2] Dennis L. Barbour,[1] Gerwin Schalk,[2,4,5,6,7] and Eric C. Leuthardt[1,2]

Departments of [1]Biomedical Engineering, [2]Neurological Surgery, and [3]Computer Science, Washington University in St. Louis, St. Louis, Missouri 63130, [4]Division of Translational Medicine, Wadsworth Center, New York State Department of Health, Albany, New York 12201, [5]Department of Neurology, Albany Medical College, Albany, New York 12208, [6]Department of Biomedical Engineering, Rensselaer Polytechnic Institute, Troy, New York 12180, [7]Department of Biomedical Sciences, State University of New York, Albany, New York 12222

High-gamma-band (>60 Hz) power changes in cortical electrophysiology are a reliable indicator of focal, event-related cortical activity. Despite discoveries of oscillatory subthreshold and synchronous suprathreshold activity at the cellular level, there is an increasingly popular view that high-gamma-band amplitude changes recorded from cellular ensembles are the result of asynchronous firing activity that yields wideband and uniform power increases. Others have demonstrated independence of power changes in the low- and high-gamma bands, but to date, no studies have shown evidence of any such independence above 60 Hz. Based on nonuniformities in time-frequency analyses of electrocorticographic (ECoG) signals, we hypothesized that induced high-gamma-band (60–500 Hz) power changes are more heterogeneous than currently understood. Using single-word repetition tasks in six human subjects, we showed that functional responsiveness of different ECoG high-gamma sub-bands can discriminate cognitive task (e.g., hearing, reading, speaking) and cortical locations. Power changes in these sub-bands of the high-gamma range are consistently present within single trials and have statistically different time courses within the trial structure. Moreover, when consolidated across all subjects within three task-relevant anatomic regions (sensorimotor, Broca's area, and superior temporal gyrus), these behavior- and location-dependent power changes evidenced nonuniform trends across the population. Together, the independence and nonuniformity of power changes across a broad range of frequencies suggest that a new approach to evaluating high-gamma-band cortical activity is necessary. These findings show that in addition to time and location, frequency is another fundamental dimension of high-gamma dynamics.

Introduction

Electrocorticography (ECoG) is the practice of recording surface cortical potentials from either epidural or subdural electrodes. Clinical use of ECoG provides a unique opportunity to study human cortical electrophysiology with high spatiotemporal resolution and signal fidelity. Many recent electrophysiological studies using ECoG and other modalities have identified gamma-band power changes as a reliable and specific phenomenon that localizes event-related neural activity in anatomy and time. At the macroscale level (defined in this work as nonpenetrating electrodes with diameters >1 mm), localized gamma-band power increases have been associated with several cognitive processes [for review of ECoG, see Jerbi et al. (2009); for magnetoencephalography (MEG), see Kaiser and Lutzenberger (2003) and Tallon-Baudry (2009); for EEG, see Herrmann et al. (2010)]. Macroscale gamma-band power increases have also been correlated with other modalities that localize cortical activity including multiunit action potential firing (Whittingstall and Logothetis, 2009) and task-related functional magnetic resonance imaging blood oxygenation level-dependent (BOLD) activations (Brovelli et al., 2005). In microscale field potential recordings, gamma-band synchrony and oscillations have been associated with many cognitive processes (Uhlhaas et al., 2009) and have been proposed as a means of neuronal communication and plasticity (Buzsaki and Draguhn, 2004; Fries et al., 2007; Colgin et al., 2009).

Given the significance of the gamma band, there are two issues this work aims to address. First, although functional distinctions between the low- and high-gamma bands have been shown in MEG and ECoG studies (Edwards et al., 2005; Wyart and Tallon-Baudry, 2008; Crone et al., 2001b), most previous macroscale research treats high-gamma power change as a uniform indicator of behavior-related cortical activity. Although differences in high-gamma spectra have been reported (Brovelli et al., 2005; Tallon-Baudry et al., 2005; Edwards et al., 2009), we are not aware of any studies that distinguish behaviors based solely on high-gamma bands. Second, there is growing interest in uniform and broadband (5–200 Hz) power increases, putatively caused by increases in asynchronous neuronal firing activity (Manning et al.,

Received Sept. 7, 2010; revised Nov. 29, 2010; accepted Dec. 3, 2010.

This work was supported by the James S. McDonnell Foundation, Higher Brain Function, the Department of Defense Grants W911NF-07-1-0415 and W911NF-08-1-0216, National Institutes of Health Grant R01-EB000856-06, and the Children's Discovery Institute. We thank our patients for their enthusiastic efforts, without which this research would not have been possible. We also thank Dr. Abraham Snyder, who provided superb insight into the understanding of these findings.

This article is freely available online through the *J Neurosci* Open Choice option.

Correspondence should be addressed to Dr. Eric C. Leuthardt, Department of Neurosurgery, Washington University in St. Louis, School of Medicine, Campus Box 8057, 660 South Euclid, St. Louis, MO 63130. E-mail: leuthardte@wustl.edu.

DOI:10.1523/JNEUROSCI.4722-10.2011

 0270-6474/11/312091-10$15.00/0

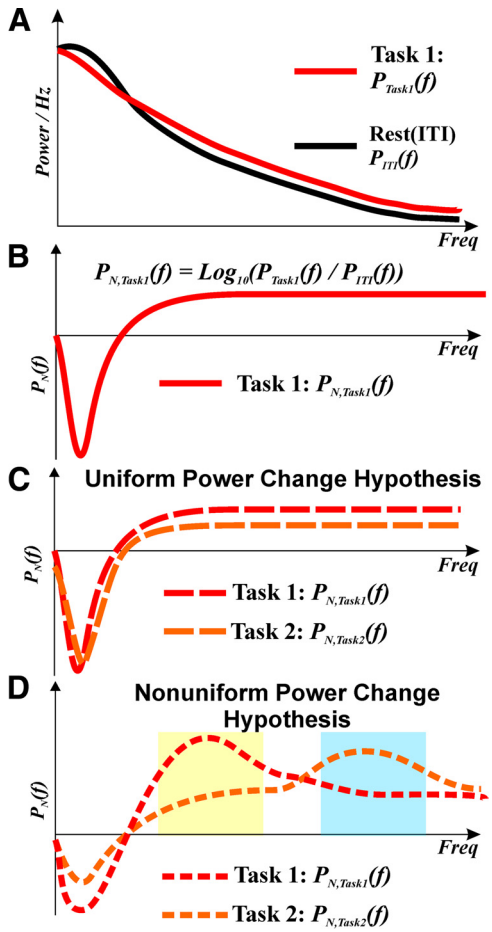

Figure 1. Schematic representations of power change paradigms. ***A***, A typical set of power spectral densities. $P_{Task}(f)$ represents the task under observation, and $P_{ITI}(f)$ represents the corresponding intertrial interval that is the basis for comparison. ***B***, The normalized power spectrum defined in equation form and illustrated schematically. This method of normalization shows the direction and magnitude of power change with reference to a resting state over a range of frequencies. ***C***, Schematic normalized spectra illustrating the hypothesis that high-gamma power change is uniform in nature. Low frequencies (μ, β, <30 Hz) tend to show power decreases for cognitive task while high frequencies have power increases. ***D***, Schematic normalized spectra illustrating the hypothesis that high-frequency power change is nonuniform. Both spectra have power changes in specific bands that distinguish one cognitive task from another.

2009; Miller et al., 2009; Miller, 2010). In light of these two items, our purpose here is to show nonuniform power modulations in sub-bands of the high-gamma range (60–500 Hz) can dissociate cognitive phases of a task or anatomic locations. This concept is illustrated in Figure 1. If ECoG can only capture uniform broadband power changes, then the induced spectra should look like those presented in Figure 1*C*. However, if ECoG can capture nonuniform power changes, presumably caused by synchronous oscillatory or suprathreshold activity, the induced spectral power change may occur in distinct frequency bands (see Fig. 1*D*, yellow and blue bars) and may dissociate cognitive behavior or anatomy.

The remainder of this work tests the hypothesis that power changes in the high-gamma band of ECoG signals are nonuniform in nature and that power modulations can be correlated with both behavior and anatomy. We show here for the first time that nonuniform power changes in 60–500 Hz ECoG signals can dissociate different cognitive tasks and anatomic locations in the manner shown in Figure 1*D*.

Materials and Methods

To test the hypothesis that the high-gamma band exhibits nonuniform power changes, we evaluated ECoG signals from six subjects undergoing treatment for intractable epilepsy. All subjects performed both auditory and visual single-word repetition tasks. Power changes between 60 and 500 Hz were studied in a variety of ways to determine whether power changes at different frequencies could distinguish phases of each task or anatomic locations. Results were consolidated across the subject population by evaluating consistency of power change in three focal anatomic areas.

Subjects. The subjects in this study underwent temporary placement of intracranial electrode arrays to identify epileptic seizure foci. All six subjects (four female) provided informed consent for the study, which had been reviewed and approved by the Washington University School of Medicine Institutional Review Board. All subjects were right handed, had no indications of bilateral speech representation, and received left hemisphere grid implants. Table 1 summarizes the subject data.

Recordings. Electrodes, manufactured by the Ad-Tech Medical Instrument Corporation, were implanted below the dura in 8 × 8 or 6 × 8 grid configurations as shown in Figure 2*A*. Individual electrodes were 4 mm diameter (2.3 mm exposed) platinum iridium discs spaced 1 cm apart (center to center) and encapsulated in SILASTIC sheets (Ad-Tech Medical Instrument Corporation, 2008). Separate four-electrode strips were implanted epidurally and facing the skull (away from the cortical surface) for biosignal amplifier ground and reference. Researchers estimated electrode coordinates in Montreal Neurological Institute (MNI) atlas space using radiographs and the "get location on cortex" technique (Miller et al., 2007). Brodmann area labels were acquired using the estimated Talairach coordinates from an on-line Talairach atlas (Lancaster et al., 2000).

Biosignal amplifiers manufactured by Guger Technologies recorded ECoG and microphone signals using a 1.2 kHz sampling rate and 24-bit resolution. Microphone signal recordings used ground and references electrically isolated from the ECoG channels to prevent interference. Signals were digitally bandpass filtered between 0.1 and 500 Hz before storage.

Experimental setup. The BCI2000 software package synchronized the single-word repetition tasks with ECoG and microphone signal recordings (Schalk et al., 2004). Stimulus periods of 4 s were interleaved between 533 ms intertrial intervals (ITIs) as shown in Figure 2*B*. Visual stimuli appeared for the whole stimulus period on a liquid crystal display monitor ~60 cm from the subject. Auditory stimuli were presented through headphones and had an average duration of 531 ms (SD, 89 ms). Stimuli for both tasks came from the same list of 36 monosyllabic English words. Subjects were instructed to repeat each stimulus word aloud into a microphone. Voice onset times (VOTs) were determined by thresholding the rectified and low-pass filtered (third-order Butterworth filter; cutoff frequency, 10 Hz) microphone signal by the mean.

Preprocessing. Researchers screened all signals for excessive noise before any analysis. Channels with excessive noise were dropped from the entire analysis. Trials with excessive environmental noise across all channels, or where speech occurred during stimulus or ITI periods, were also excluded from analysis. After dropping noisy channels and trials, all signals were re-referenced to a common average reference.

Power spectral densities. Discrete estimates of spectral power for cognitive tasks used autoregressive methods. The estimated power spectral densities (PSDs) [$P(f, C, Tr, w)$, where f is the frequency bin, C is the channel, Tr is the trial, and w is the temporal window] were calculated using the Yule–Walker method and a model order of 50 (Kay and Marple, 1981). The model order was selected to subjectively balance PSD smoothness with the ability to precisely detect known sinusoidal noise peaks (environmental noise). Comparison of normalized PSDs estimates across cognitive tasks between the autoregressive method and the fast Fourier transform are shown in supplemental Figures 1 and 2 (available at www.jneurosci.org as supplemental material) and demonstrate qualitative and quantitative agreement in the spectral estimates. Individual frequency bin spectral estimates were evaluated at 2 Hz centers, between 2 and 500 Hz, by averaging the response of the autoregressive model

Table 1. Subject data

Subject	Age/sex	Hand	Cognitive capacity	Grid location	Epileptic focus	Number of trials per task
1	15/female	R	Normal	Left F/P	Left temporal	72
2	44/male	R	Avg to high avg	Left F	Left orbitofrontal	72
3	27/male	R	Low average (FSIQ, 89; VIQ, 86; PIQ, 96)	Left F/P	Right mesial parietal	180
4	58/female	R	High avg (FSIQ, 116)	Left F/P	Superior frontal gyrus	216
5	49/female	R	Avg (FSIQ, 100)	Left F/T	Anterior temporal	216
6	42/female	R	Low avg (FSIQ. 81)	Left F/T/P	Anterior temporal/amygdala/ hippocampus	109

FSIQ, Full-scale intelligence quotient; VIQ, verbal intelligence quotient; PIQ, performance intelligence quotient; R, right; F, frontal; P, parietal; T, temporal; avg, average. All grids were left sided.

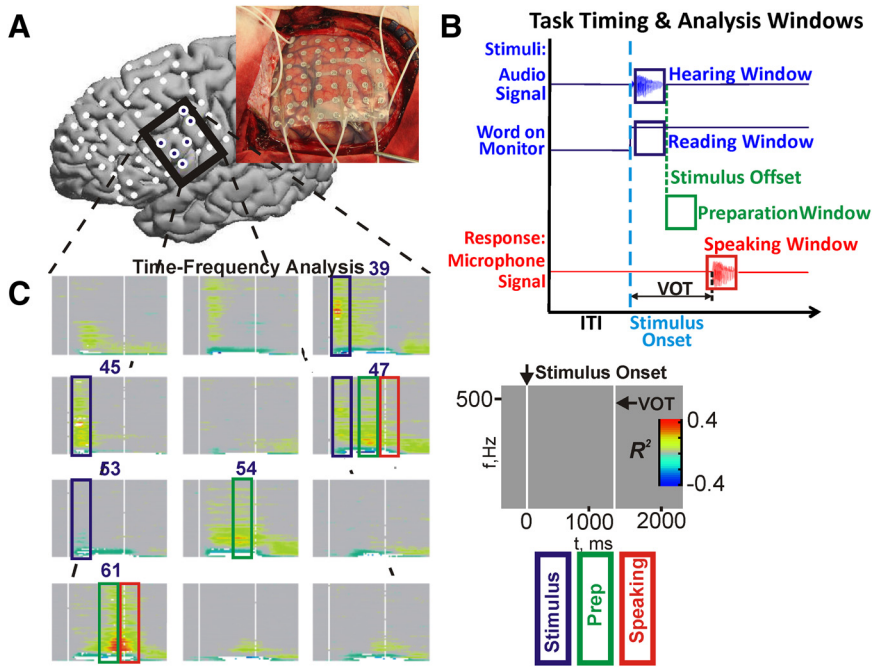

Figure 2. Experimental setup and time-frequency analysis of ECoG signals. ***A***, Photograph of implanted ECoG electrodes and corresponding localization on the MNI model brain. Filled electrodes represent electrodes of interest in ***C***. ***B***, The timing of the two different experimental paradigms. Single-word stimuli were presented either aurally or visually. Analysis windows for hearing and reading were cued to stimulus onset, preparation analysis windows were cued to stimulus offset, and windows for speaking were cued to voice onset detected from microphone signal (see Materials and Methods for time delay and duration). ***C***, Typical time-frequency plots for the auditory repeat paradigm showing statistically significant ($p < 0.001$) coefficient of determination (R^2) values. This region of 12 electrodes is highlighted as an exemplar region. All nonsignificant R^2 values are grayed out. Six electrodes of interest are numbered and correspond to the filled electrodes in ***A***. The colored rectangles highlight notional analysis windows with interesting nonuniform power change patterns. Keys for analysis window rectangles and time-frequency plot template are shown to the right.

transfer function at 10 samples spaced 0.2 Hz apart and centered on each frequency bin. Cognitive task and corresponding ITI PSDs in each trial are the mean of five spectral estimates using 250 ms windows with 75% overlap covering a 500 ms block of samples, as described in Equation 1. Each block of samples was time cued to the stimulus onset, stimulus offset, or VOT in each trial. Blocks of samples for stimuli started 100 ms after onset. Preparatory period blocks commenced at auditory stimulus offset and productive speech blocks began 100 ms before the VOT. The block timing parameters were selected empirically after reviewing time-frequency analyses as seen in Figure 2*C*.

$$P_{\text{activity}}(f,C,Tr) = \frac{1}{5}\sum_{w=1}^{5} P(f,C,Tr,w) \quad (1)$$

Time courses of power in specific frequency bands that span multiple cognitive tasks were calculated using the complex Gabor wavelet transform with time-domain standard deviations of either $4/f_c$ ($f < 120$ Hz) or $16/f_c$ ($f > 120$ Hz), where f_c is the center frequency of the wavelet (Bruns, 2004). The transform magnitude was downsampled by computing the mean in nonoverlapping windows of eight samples. The eight-sample window size was selected to synchronize the time course of power in the ECoG signal with the stimulus timing from the BCI2000 software. The downsampled time course data are referred to using the symbol, $P_{DS}(t, f, C, Tr)$, where t is the time sample in the downsampled series, and the other variables are as stated previously.

Dissociation bands. Sets of frequency bands that dissociated either cognitive task or anatomy were analyzed in several ways. These bands were first detected using normalized spectra, $P_{N,\text{ activity 1}}(f, C, Tr)$, described in Figure 1*B* and Equation 2.

$$P_{N,\text{activity 1}}(f,C,Tr) = \log_{10}\left[\frac{P_{\text{activity 1}}(f,C,Tr)}{P_{\text{ITI}}(f,C,Tr)}\right] \quad (2)$$

This normalization technique helps remove the nonstationary changes in the ECoG signal and environmental noise that occur on short (~4 s) time scales, equalizes the scales for power increases and decreases, and provides a basis to compare power changes to the schematic illustrations in Figure 1. An artifact in the normalization method is the presence of downward-pointing spikes in the normalized power spectrum (see Figs. 3, 4). Since the power of the environmental noise was relatively constant and in general greater than the cortical power in the signal, the difference between cognitive task and rest was negligible at the noise frequencies; therefore, a narrow slice of the normalized spectra is not significantly different from zero (ITI power level).

The next step in identifying dissociation bands was to identify specific frequency bands with statistically significant differences in normalized power. Confidence intervals on the mean normalized power level were calculated for each cognitive task, channel, and frequency bin across all trials. For each pair of cognitive tasks, frequency bins were identified as statistically different if the means for each task had nonoverlapping confidence intervals at one of three levels (95, 99, or 99.9%). If at least three contiguous frequency bins (each 2 Hz wide) had nonoverlapping confidence intervals, a single frequency band with a statistically significant difference in power was identified. Using the individual bands with statistically significant differences in power, pairs of dissociation bands were defined as follows. For a given channel and pair of cognitive tasks, a pair of dissociation bands was counted if (1) in one frequency band, the confidence intervals were nonoverlapping and the mean normalized power during cognitive task A was significantly greater than the mean power during cognitive task B, and (2) in the second frequency band, the confidence intervals were nonoverlapping and the mean normalized power during A was less than the mean power during B. In this case, these high-gamma sub-bands dissociate the two cognitive tasks. The schematic illustration in Figure 1*D* is an example of a pair of dissociation bands. Using an analogous test, dissociation bands between pairs of electrodes during a single cognitive task can also be detected. In this case, the high-gamma bands dissociate the two anatomic locations.

After identifying the dissociation bands, single-trial and time course data were also evaluated to further confirm the consistency of the power changes. To show the consistency of the power changes across the course of the experiments, the normalized spectra, $P_{N,\,\text{activity}}(f, C, Tr)$, from 30–500 Hz for every individual trial were plotted. The boundaries of the dissociation bands are indicated to show the spectral regions that dissociated the cognitive tasks (or locations) of interest. To visualize the temporal dynamics of power change in the dissociation bands, the time courses of normalized power change for each cognitive task are shown. In a manner similar to that described for the normalized spectra, time courses were normalized by dividing each time sample by the mean power in the preceding ITI and taking the logarithm, as shown in Equations 3 and 4. One second windows of the normalized, downsampled power in each frequency band $P_{N,\,DS}(t, f, C, Tr)$ were aligned to either stimulus onset (hearing or reading), stimulus offset (preparation), or voice onset (speaking). Time course plots show the mean across all trials of the normalized, downsampled power with 95% confidence intervals to illustrate the statistical significance of the difference in power over time.

$$\bar{P}_{DS,\text{ITI}}(f,C,Tr) = \frac{1}{N_{\text{ITI}}}\sum_{t=0}^{N_{\text{ITI}}-1} P_{DS,\text{ITI}}(t,f,C,Tr) \quad (3)$$

$$P_{N,DS,\text{activity1}}(t,f,C,Tr) = \log_{10}\left[\frac{P_{DS,\text{activity1}}(t,f,C,Tr)}{\bar{P}_{DS,\text{ITI}}(f,C,Tr)}\right] \quad (4)$$

Cortical activation plots. Summaries of power change across the population of six subjects show consistency of power change over a wide range of frequencies. These figures show the proportion of channels within three focal anatomic areas [Broca's area, sensorimotor cortex, and superior temporal gyrus (STG)] that had statistically significant power changes in each specified cognitive task by frequency. These plots show trends in consistency of power change by frequency bin across subjects without allowing the actual magnitude of the power change to influence the shape of the plots. Consistency of power change was evaluated using the coefficient of determination (R^2), which quantifies the percentage of variance in each frequency bin attributed to the difference between a cognitive task and rest. The statistical significance of each R^2 was determined using the p value of a one-way, balanced ANOVA. To correct for multiple comparisons in each plot, a false discovery rate (FDR) correction was applied as follows (Benjamini and Hochberg, 1995). In each bar plot, the p values for all frequency bins between 60 and 500 Hz from the electrodes in the anatomic area of interest and the cognitive task under study were collectively corrected for multiple comparisons using a false discovery rate level of 0.001. After correction, significant p values were counted by frequency bin for each electrode in the anatomic area of interest and cognitive task. These counts were converted to a percentage by dividing by the total number of electrodes within the corresponding anatomic area and then shown as bar plots. Cortical activation bar plots show the percentage of electrodes with statistically significant power changes in each frequency bin for each combination of anatomic area and cognitive task.

The shape of the bar plots helped evaluate the difference in the proportion of frequency bins with significant power changes between anatomic locations and cognitive tasks. These differences were quantified using two-sample Kolmogorov–Smirnov tests. For each plot, the counts of electrodes with significant p values (after FDR correction) at each frequency bin were converted to actual data samples. For example, if three electrodes within a region were significant at 72 Hz, three 72's were added to the set of data samples. The sets of samples from two cortical activation bar plots were then tested to determine whether they came from the same distribution ($p < 0.05$). The difference in shape provides a means to evaluate the differences in power change in focal anatomic locations across the population of subjects.

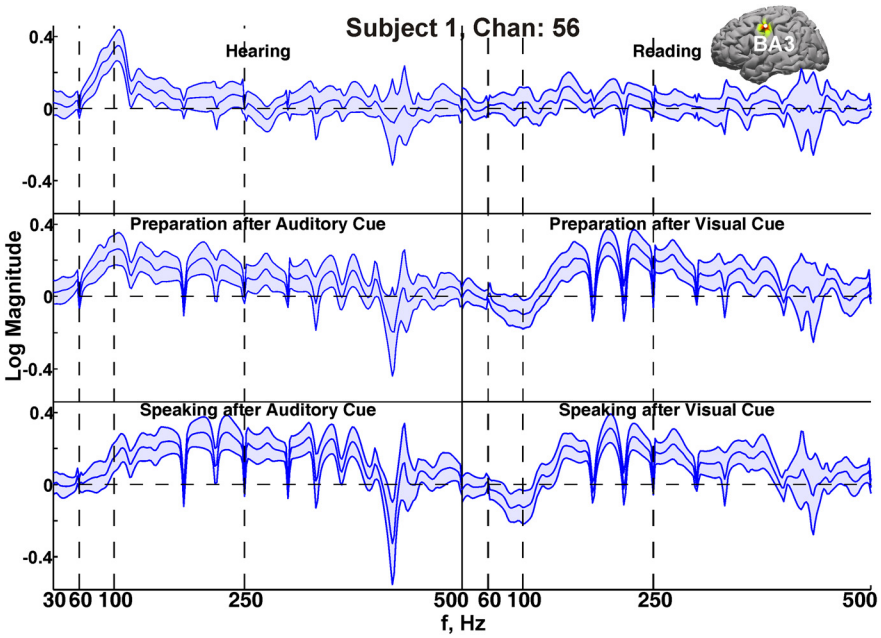

Figure 3. Exemplar normalized spectra illustrate that high-gamma-band power changes are nonuniform and distinct between tasks. The blue center line is the mean normalized spectra across 71 trials. The shaded area encapsulates the 95% confidence intervals. Vertical dashed lines at 60, 100, and 250 Hz outline typical gamma-band analysis boundaries. Frequencies with normalized spectra greater than zero indicate behavior-induced power increases, whereas values less than zero reflect power decreases. Note that for all six cognitive tasks, the patterns of spectral power change are unique across a wide range of frequencies. Each cognitive task has different bandwidths of frequencies that are statistically different from rest, and in some bands the direction (sign) of power change between cognitive task reverses (e.g., 60–120 Hz hearing vs speaking after visual cue). The sharp downward spikes are the result of environmental noise components that do not change in magnitude between cognitive task and ITI.

Results

Behavioral data

Each of the six subjects performed both the auditory and visual versions of the single-word verbal repetition paradigm. The mean VOT across subjects for the auditory task was 998 ms (SD, 453 ms), and for the visual task it was 825 ms (SD, 463 ms). These statistics are on the same order of magnitude as those from studies using similar tasks (Church et al., 2008) and indicate that the subjects did not have difficulty performing the experimental tasks.

High-gamma-band power changes are nonuniform and extend up to 500 Hz

Each of the six subjects in this study had electrodes with behaviorally induced power changes that were nonuniform, but were instead concentrated in specific frequency bands. These nonuniform power changes are most visible in the normalized log magnitude spectra as shown for an exemplar subject and single electrode in Figure 3. In this example, there are marked differences between the spectra for the six different cognitive tasks, especially in the frequency bands between 60 and 120, 122 and 400, and 480 and 500 Hz. This electrode responded strongly to the auditory stimulus between 60 and 160 Hz, however, the visual stimulus response had a much smaller magnitude and was statis-

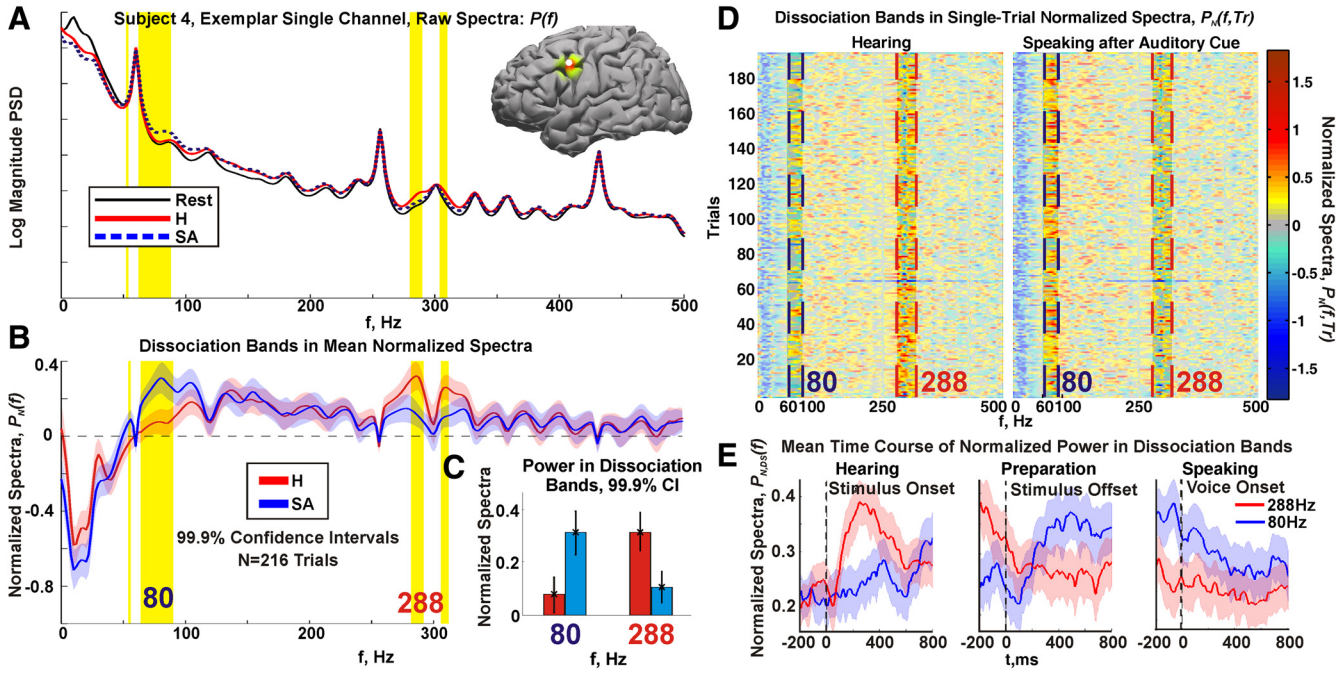

Figure 4. The dynamics of power in dissociation bands. ***A***, Exemplar mean raw PSDs for rest and two cognitive tasks for $N = 216$ trials. H, Hearing; SA, speaking after auditory cue. Yellow bands around 80 and 288 Hz highlight high-gamma frequency bands that dissociate the two tasks. ***B***, Mean normalized spectra (solid lines) with 99.9% confidence intervals (shaded areas) show differences in the spectral power change patterns as averaged over all trials. Nonoverlapping confidence intervals and a reversal in the relationship between power levels in the two highlighted frequency bands illustrate a pair of dissociation bands. Note also that behaviorally induced power change is significantly different from rest as high as 500 Hz. ***C***, Bar plot with 99.9% confidence intervals illustrates the statistical significance of the difference in normalized power between the two cognitive tasks for the dissociation bands in ***B***. This format is used for other subjects in Figure 5. ***D***, Single-trial normalized spectra for the single electrode and two cognitive tasks in ***A–C*** illustrate the consistency of power change in the dissociation bands across trials. These plots show that normalized spectra in the dissociation bands are not dominated by outliers in any single trial. The color intensity outside of the dissociation bands is subdued to highlight activity in the bands under study. ***E***, Time courses of power in the dissociation bands from ***A–C***. The mean downsampled and normalized power level for each frequency with 95% confidence intervals shows that during over the course of the experiment, power levels in the two dissociation bands reverse.

tically different than rest primarily between 140 and 160 and 200 and 230 Hz. The two speaking tasks had similar responses across a wide range of frequencies between 90 and 400 Hz, with notable differences in the 80–130 and 480–500 Hz bands. The two preparatory periods appear to be a blend between the spectral patterns of the stimuli and vocal response. All subjects had electrodes that exhibited nonuniform power changes in the normalized spectra across various cognitive tasks. In many cases, the nonuniformities in the high-gamma band were specific enough to dissociate different cognitive tasks and anatomic locations.

High-gamma dissociation bands quantify nonuniformity in spectral power change

We quantified the nonuniformity of power change in high-gamma frequencies by identifying dissociation bands. When the independence of power change in two different high-gamma frequency bands can dissociate cognitive tasks or anatomic locations, they are identified as "dissociation bands," as illustrated in Figure 4, *B* and *C*, and as follows. In the frequency band around 80 Hz, the confidence intervals on normalized power change are nonoverlapping and "speaking after auditory cue" has a greater normalized power than hearing. In the second highlighted frequency band, around 288 Hz, again the confidence intervals are nonoverlapping, but hearing induces a greater power change than speaking after auditory cue. Additionally, because the independence of low gamma (30–60 Hz) and high gamma (>60 Hz) has been reported previously, we also constrained our search for dissociation bands to the frequency range between 60 and 500 Hz (Edwards et al., 2005; Crone et al., 2001a). The single-trial normalized spectra in Figure 4*D* illustrate the consistency of the dissociation band phenomena. Over 216 trials, the normalized spectra show that for hearing, the 288 Hz band has a consistently higher magnitude of power change (warmer colors) than speaking after the auditory cue. Likewise, in the 80 Hz band, the "speaking after auditory cue" normalized spectra have consistently larger magnitudes of power change (warmer colors) than hearing. The reversal in normalized power is also evident in the time course of power in the two dissociation bands. Figure 4*E* shows the mean and 95% confidence intervals of the normalized, downsampled spectra for the frequency bands around 80 and 288 Hz. Over the course of the three cognitive tasks in the auditory repetition paradigm, the power levels reverse toward the end of the preparatory task and just before voice onset. From these three views of the spectral power, it is evident the power levels at this electrode are independent enough to dissociate the different tasks in these two high-gamma sub-bands.

We identified several pairs of dissociation bands for each subject. The single-electrode dissociation bands represent single anatomic locations where different high-gamma bands distinguish cognitive tasks. We also tested for pairs of electrodes that had different high-gamma bands that dissociated anatomic locations during the same cognitive task. Figure 5 contains exemplar single or multielectrode dissociation bands for all six subjects. Five of the six subjects had single-electrode dissociation bands that distinguished strictly cognitive task. The second subject's exemplar comes from a pair of electrodes that dissociated solely anatomic locations. Supplemental Figure 3 (available at www.jneurosci.org as supplemental material) contains the normalized spectra associated with each subject's exemplar dissociation bands. Although many of the dissociations were caused by differences in the mag-

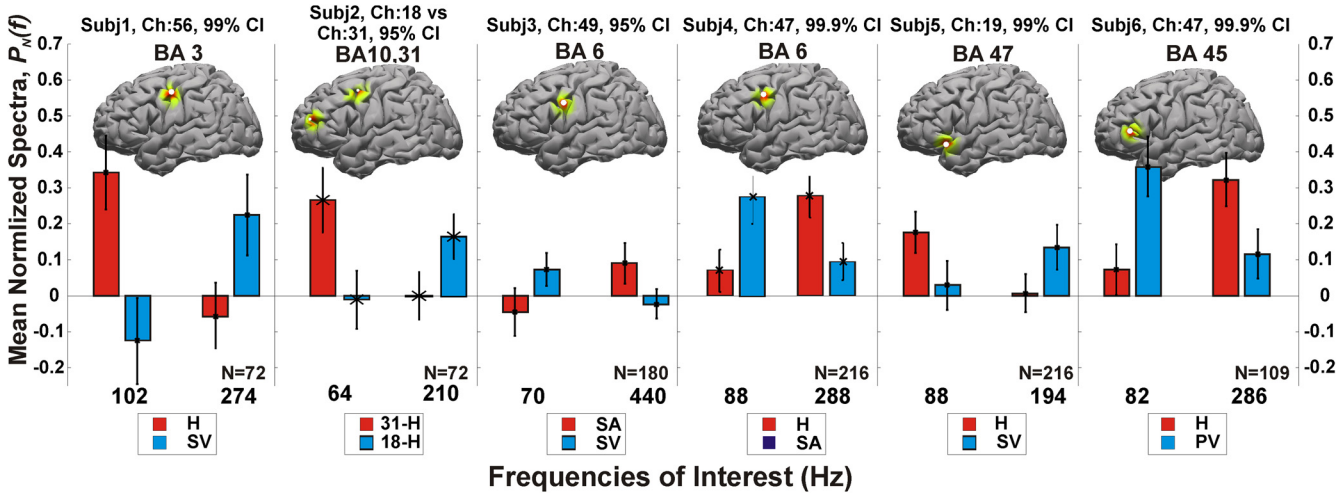

Figure 5. Exemplar dissociation bands for all six subjects. See Figure 4 for the derivation of individual bar plots. The electrode(s) of interest, confidence intervals (CIs), associated BA labels, and cortical location on the MNI model brain are shown above each bar plot for reference. Subject 2 did not have single electrodes with dissociation bands, and therefore the exemplar shows power change reversals between two electrodes during the same cognitive task. H, Hearing; PV, preparation after visual cue; SA, speaking after auditory cue; SV, speaking after visual cue.

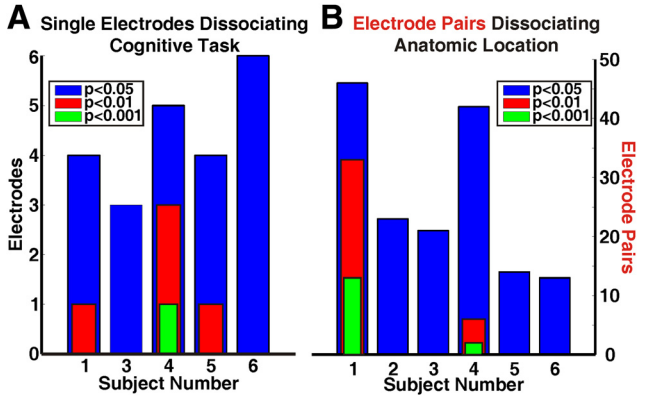

Figure 6. Summary of quantities of dissociation bands across the subject population. ***A***, ***B***, Each bar shows the number of single electrodes (***A***) or electrode pairs (***B***) with dissociation bands for each subject by *p* value. ***A***, This chart quantifies the number of single electrodes with significant power changes in different high-gamma frequencies that dissociated two or more cognitive tasks. ***B***, This chart quantifies the number of electrode pairs in which different high-gamma frequencies dissociated anatomic locations during the same cognitive task.

nitude of normalized power increases, there were dissociation bands that were caused by significant power decreases. Supplemental Figure 4 (available at www.jneurosci.org as supplemental material) summarizes the percentages of single-electrode dissociation bands in which at least one of the dissociating frequency bands had a significant power decrease. Figure 6 contains a quantitative summary of the electrodes and electrode pairs with dissociation bands by individual subject and statistical strength. The numbers of single electrodes with high-gamma bands dissociating cognitive task are plotted in Figure 6*A*, whereas Figure 6*B* summarizes the number of electrode pairs that dissociate anatomic location. The statistics across this group of subjects show that the independence of power change in sub-bands across the range of high-gamma frequencies is not an anomaly. The pervasive occurrence of dissociation bands especially within data from single electrodes across this population of subjects indicates that ECoG signals can capture population dynamics that produce nonuniform power changes across the high-gamma band up to 500 Hz.

Cross-subject analysis by anatomy and cognitive task

Evaluating spectral power modulation across subjects shows that power changes occur nonuniformly even within small anatomic regions. Three cortical regions [left sensorimotor cortex, Brodmann areas (BAs) 1–4; Broca's area (BAs 44–45), and left STG (BAs 22, 42)] have all been implicated in functional imaging studies using similar language tasks and were therefore selected for more detailed analysis (Church et al., 2008). In Figure 7, for each combination of cortical region and cognitive task, bar plots show the percentage of electrodes within that region from all six subjects that had statistically significant R^2 values (FDR correction level, 0.001) at each frequency. These plots provide a means to evaluate the significance and consistency of spectral power change across the subject population and have the appearance of a pseudospectrum, but allow an evaluation across the subject population without permitting individual differences in the magnitude of power change to affect the shape of the plot. By confining the scope to three anatomical areas and four cognitive tasks, we can visualize trends in high-gamma-band power change across the entire population of subjects. In these plots, high numbers at a given frequency indicate that a high percentage of electrodes within a specific cortical region had consistent power changes across subjects during a specific cognitive task. If power changes occurred uniformly across frequencies for all subjects as in Figure 1*C*, the cortical activation plots would be flat. On the other hand, if power changes are confined to specific bands, then the shape of the activation plots should have variation because of band-specific power changes from different electrodes within the anatomic area or from individual differences between subjects. The results show that power changes occur nonuniformly even within small cortical regions.

There are three trends in the consolidated cortical activation plots in Figure 7 that support the hypothesis that high-gamma power change occurs nonuniformly across a wide range of frequencies. First, many single activation plots exhibit multiple peaks (e.g., sensorimotor cortex while speaking after auditory cue, Broca's area while speaking after visual cue, STG while speaking after auditory cue). These peaks indicate the presence of statistically significant power changes in different frequency bands during the same cognitive task and within the same cortical region across the population of subjects. Second, within cortical

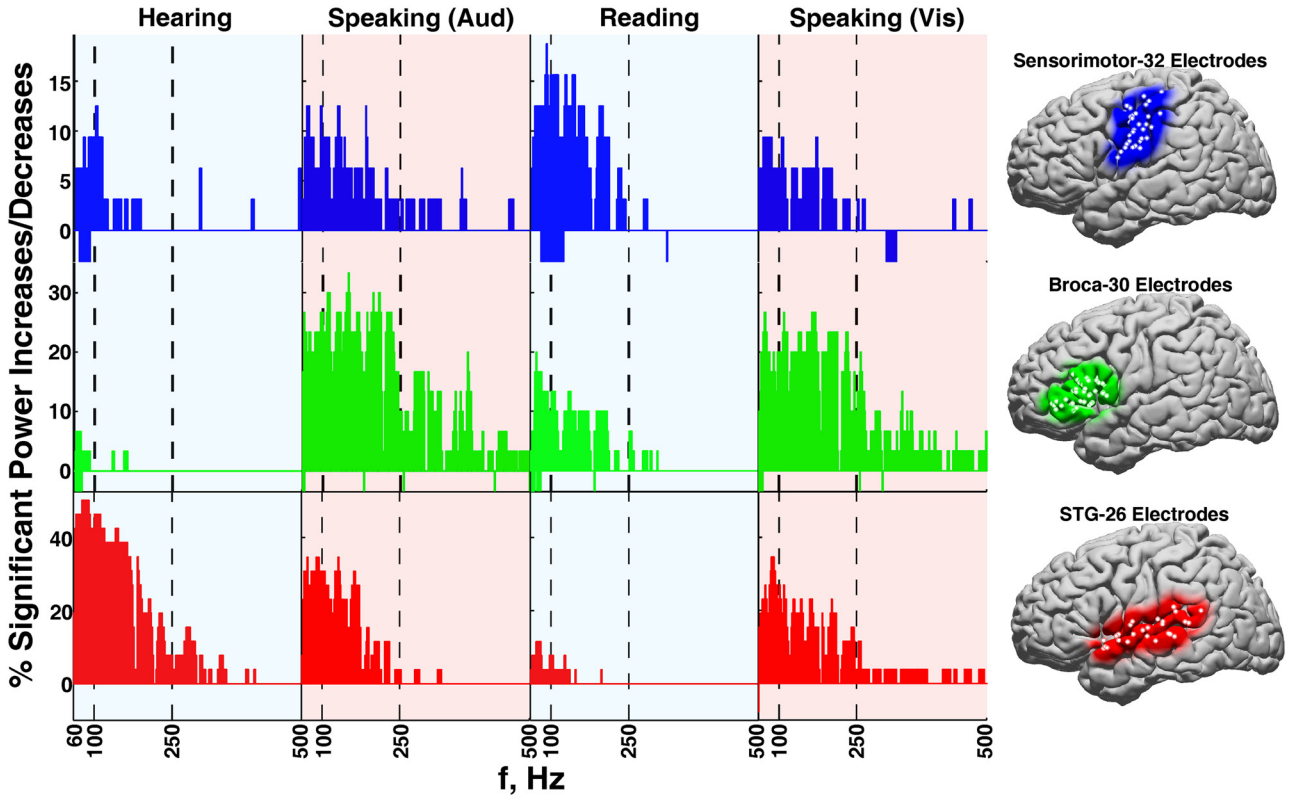

Figure 7. Consolidated cortical activation plots for the population of six subjects. Positive numbers indicate percentage of electrodes with statistically significant ($p < 0.001$, FDR corrected for multiple comparisons) power increases. Negative numbers correspond to power decreases. Rows of activation plots correspond to cortical regions, and columns to cognitive tasks. Markers at 60, 100, and 250 Hz are typical gamma or high-gamma analysis boundaries. All subject electrodes for each cortical region of interest are plotted on the MNI model brain for reference. Multiple peaks per plot, shifts in percentage of cortex with significant power changes across frequency bands, and changes in bandwidths with significant power changes within cortical populations are all evidence of nonuniform power modulation in high-gamma bands (60–500 Hz).

regions (Figure 7, single rows), cognitive tasks have either distinct active bandwidths or shifts in frequency band representations within similar active bandwidths. As an example, within Broca's area, reading is distinguished from the other three tasks by active frequency range (60–300 vs 60–500 Hz). In contrast, hearing and speaking after visual cue have similar active bandwidths (60–500 Hz), but are separable by the different proportions of cortex engaged across the range of active frequencies. For example, during speaking after the auditory cue, there are peaks in the histograms around 112, 150, 200, 286, 380, and 450 Hz, whereas during speaking after the visual cue, the peaks in the histograms appear at 70, 110, 170, 290, and 338 Hz. This second trend explicitly shows that the cortical region activates at different frequencies in a behavior-dependent manner. If power change occurred uniformly, and the only variable within these plots was the number of electrodes within the population that was active, all histograms would be flat with differing heights according to the percentage of electrodes with significant power change. The third trend is that for any given cognitive task, there is variation in the active bandwidths between the three cortical regions. In other words, there does not appear to be a unified activation bandwidth across cortical regions for a specific cognitive task. As a quantitative measure of the differences identified by the second and third trends, we evaluated the statistical significance of the differences in bar plot shape using two-sample Kolmogorov–Smirnoff tests (for detailed results, see supplemental Table 1, available at www.jneurosci.org as supplemental material). Overall, these tests indicate that 83% of cortical activation plot comparisons (55 of 66 comparisons) are statistically distinct ($p < 0.05$). These three trends were also present in individual subjects. Supplemental Figure 5 (available at www.jneurosci.org as supplemental material) shows cortical activation plots for a single subject exemplar that illustrates these same three trends.

Discussion

This study demonstrates, in a population of six subjects, that ECoG surface cortical potentials have nonuniform induced power changes in high-gamma sub-bands. Dissociation bands showed that sub-band power modulations were independent enough to dissociate cognitive tasks and anatomic locations. Moreover, when power modulations were summated across subjects, there were persistent behaviorally and anatomically dependent trends. Neither the dissociation bands nor the peaks in the cortical activation plots can be caused by uniform power increases. These findings are consistent with previously published results from many modalities and significantly alter the perspective on the extent and nature of high-gamma-band power changes in macroscale electrophysiology.

Evidence of nonuniform high-gamma power changes in previously published literature

Previous studies have demonstrated that physiologically relevant cortical power changes can occur at various high frequencies. Single-unit local field potential recordings in rodents have reported gamma oscillations up to 150 Hz (Sirota et al., 2008). Macroscale recordings from ECoG, EEG, and MEG have also reported the independence of cortical power changes between low-gamma (~30–60 Hz) and high-gamma (>60 Hz) bands

(Herculano-Houzel et al., 1999; Edwards et al., 2005; Wyart and Tallon-Baudry, 2008; Crone et al., 2001a). We confirmed this distinction by identifying several additional single and multielectrode dissociation bands between 30 and 500 Hz (supplemental Fig. 6*A*,*B*, available at www.jneurosci.org as supplemental material). Our results (Figs. 5, 6) further extend this subparcellation to the high-gamma band above 60 Hz. Although many studies have identified unitary power changes in the high-gamma band associated with cognitive behavior, the results presented here show that there is behavioral information encoded in sub-bands above the 60 Hz marker.

Gamma-band activity has been attributed to a variety of cellular mechanisms, both normal and pathologic. Low-gamma (30–60 Hz) oscillations are purportedly caused by alternating excitatory and inhibitory postsynaptic potentials (Sukov and Barth, 1998). The physiological underpinnings of oscillations between 60 and 200 Hz are less clear. Single-unit studies in nonhuman primate somatosensory cortex have correlated local field potentials between 60 and 200 Hz and average firing rates (Ray et al., 2008). EEG studies in primate primary visual cortex have shown that gamma power (30–100 Hz) coupled to delta phase (2–4 Hz) can predict multiunit firing rates (Whittingstall and Logothetis, 2009). Higher-frequency oscillations (up to 600 Hz) caused by peripheral nerve stimulation have been reported in nonhuman primate epidural and single-unit recordings (Baker et al., 2003) and human scalp EEG/MEG (Curio, 2000). Higher oscillatory frequencies (200–600 Hz) appear to be correlated with summated action potential spiking (Jones et al., 2000; Baker et al., 2003). It may be that the 60–200 Hz range of the high-gamma-band power increases are associated with asynchronous increases in multiunit firing rates, whereas gamma-band power above 200 Hz indicates synchronous firing activity. In addition to natural physiological processes, evidence of high-frequency "fast ripples" (250–500 Hz) have been reported in human epileptic hippocampus (Bragin et al., 2002). Since all subjects in this study underwent treatment for epilepsy, it is possible that some power change patterns in our data are pathologies of the disease. However, the strength of the statistical tests used to correlate power changes with specific cognitive tasks as well as the single-trial and time course data indicate that these high-frequency power changes are not random occurrences. Together, these studies show that there are physiological bases for power changes between 60–500 Hz.

Absence of nonuniform high-frequency power changes in previously published literature

There are several legitimate reasons that previous ECoG studies have not identified distinct, nonuniform high-gamma power change patterns that dissociate cognitive tasks or locations. Choice of behavioral task, data collection method, or analysis technique could obscure these differences. Many ECoG studies of language use experimental paradigms designed to illuminate cortical changes caused by subtle differences in cognitive behaviors (e.g., phonological processing, semantic processing, lexical processing, etc.). The paradigms often focus on cortical responses to input stimuli with relatively simple behavioral responses (e.g., button press) (Mainy et al., 2008) or passive stimulation alone (Edwards et al., 2005). Although differences in high-gamma activity may have been present, they may have been subtle or considered irrelevant. Additionally, studies of relatively simple motor tasks (e.g., hand clasping, finger movements) that have reported uniform power increases correlated with movement (Miller et al., 2009) may involve different physiologies. Functional imaging studies of finger movements implicate much smaller regions of BOLD signal change (Cunnington et al., 2002) than those for the language tasks studied here (Church et al., 2008). The difference between a more focal versus a more networked cortical process may result in genuinely different electrophysiological responses. Thus, broadband responses to motor tasks may also be behavior and location specific, but may not necessarily generalize to other tasks or cortical areas.

Signal-to-noise ratios and frequency analysis techniques may also explain why other research has not reported the high-frequency behavior shown here. The raw power spectral density of electrical cortical activity drops off geometrically in proportion to the observation frequency (Nunez and Srinivasan, 2006); therefore, when analyzing high frequencies, practices that improve signal-to-noise ratio are critical. Recordings for this work used intracranial and noncortical (skull-facing) reference electrodes, which are less susceptible to noise than scalp or cortical electrodes. Biosignal amplifiers used in this study have 24-bit analog-to-digital converters. Equipment with lower precision (using fewer bits) will have higher quantization noise levels, which may obscure low power fluctuations at high frequencies. Linear time-frequency analysis techniques (wavelet and Fourier transforms) inherently trade time resolution for frequency resolution (Hlawatsch and Boudreaux-Bartels, 1992). Selecting analysis parameters that favor fine time resolution can obscure narrowband changes because of coarse frequency resolutions at higher ranges.

Support from neurophysiological studies of human language

Overall, cortical functions reported in human language studies using other modalities support the behavior-related patterns of cortical activity in Figure 7. Sensorimotor cortex had strong activations in all four cognitive tasks. Although its role during receptive speech is the subject of much debate (Scott et al., 2009), our findings are in line with likely roles of phonetic encoding, formulation of motor articulatory plans, and other motor control activities (Petersen and Fiez, 1993; Salmelin, 2007; Towle et al., 2008) as well as multisensory integration (Ghazanfar and Schroeder, 2006). Broca's area had robust cortical activations during speaking tasks, moderate activations during reading, and minimal activations during hearing. These activations are likely attributable to the graphophoneme conversion process during reading (Jobard et al., 2003; Salmelin, 2007) and late prearticulatory responses in preparation for speech (Indefrey and Levelt, 2004; Towle et al., 2008), which may occur late in the hearing phase. The activations in left STG were strongest during hearing and speaking but were minimal during reading. Primary auditory perception, phonological processing (Binder et al., 2009), and self-monitoring (Demonet et al., 2005) are likely the functions causing activations during hearing and speaking. Although electrophysiological studies have reported high-frequency power increases during reading associated with lexical and semantic processing (Salmelin, 2007; Mainy et al., 2008), the weaker response during reading in Figure 7 is most likely because the read and repeat paradigm used here required little lexical or semantic processing.

Alternative explanations

Although there is agreement between our results and corresponding findings in microscale high-gamma studies and language studies from multiple modalities, we acknowledge there are possible alternative explanations. The normalization technique used here removes noise characteristics that may change

over time; however, as a result, the ITI spectra are explicitly included in the comparisons between tasks. Therefore, it is possible that some of the dissociation band phenomenon reported here could also have been caused by differences in the ITI spectra either between experimental tasks (single electrodes) or between pairs of electrodes during the same cognitive task. There is a finite precision in the electrode registration method used here (~1 cm) that directly affects Brodmann area assignment (Miller et al., 2007). Additionally, it is well known that there are significant individual differences in the organization of cortical language areas (Ojemann et al., 1989). Regardless of possible inaccuracies in Brodmann area categorization or subject-specific differences in functional anatomy, the vast agreement between the existing language literature and our results supports the credibility of the results presented here and amplifies the dissociation band findings.

In conclusion, these findings indicate a new approach is necessary to evaluate high-gamma range macroscale electrophysiology. In addition to time and location of power changes, the specific frequency band within the high-gamma range is another fundamental dimension of cortical electrophysiology. Though the cellular underpinnings of these phenomena require further study, we posit that these distinct, frequency-specific changes represent a mixture of asynchronous increases in multiunit activity as well as synchronous oscillatory activity and action potential firing. Regardless of the source of these spectral nonuniformities, the discovery of frequency diversity in the high-gamma range provides the opportunity to explore the dynamics of these narrow frequency bands and their behavioral and neuronal correlates, which may better facilitate the continuing synthesis of cellular, ensemble, and behavioral neuroscience.

References

Ad-Tech Medical Instrument Corporation (2008) 2008 Product catalog—epilepsy and neurosurgery product guide. Racine, WI: Ad-Tech Medical Instrument Corporation.

Baker S, Gabriel C, Lemon R (2003) EEG oscillations at 600 Hz are macroscopic markers for cortical spike bursts. J Physiol 550:529–534.

Benjamini Y, Hochberg Y (1995) Controlling the false discovery rate: a practical and powerful approach to multiple testing. J R Stat Soc Series B Stat Methodol 57:289–300.

Binder JR, Desai RH, Graves WW, Conant LL (2009) Where is the semantic system? A critical review and meta-analysis of 120 functional neuroimaging studies. Cereb Cortex 19:2767–2796.

Bragin A, Wilson CL, Staba RJ, Reddick M, Fried I, Engel J Jr (2002) Interictal high-frequency oscillations (80–500 Hz) in the human epileptic brain: entorhinal cortex. Ann Neurol 52:407–415.

Brovelli A, Lachaux JP, Kahane P, Boussaoud D (2005) High gamma frequency oscillatory activity dissociates attention from intention in the human premotor cortex. Neuroimage 28:154–164.

Bruns A (2004) Fourier-, Hilbert- and wavelet-based signal analysis: are they really different approaches? J Neurosci Methods 137:321–332.

Buzsaki G, Draguhn A (2004) Neuronal oscillations in cortical networks. Science 304:1926–1929.

Church JA, Coalson RS, Lugar HM, Petersen SE, Schlaggar BL (2008) A developmental fMRI study of reading and repetition reveals changes in phonological and visual mechanisms over age. Cereb Cortex 18:2054–2065.

Colgin L, Denninger T, Fyhn M, Hafting T, Bonnevie T, Jensen O, Moser M, Moser E (2009) Frequency of gamma oscillations routes flow of information in the hippocampus. Nature 462:353–357.

Crone NE, Boatman D, Gordon B, Hao L (2001b) Induced electrocorticographic gamma activity during auditory perception. Clin Neurophysiol 112:565–582.

Cunnington R, Windischberger C, Deecke L, Moser E (2002) The preparation and execution of self-initiated and externally-triggered movement: a study of event-related fMRI. Neuroimage 15:373–385.

Curio G (2000) Linking 600-Hz "spikelike" EEG/MEG wavelets ("sigma-bursts") to cellular substrates: concepts and caveats. J Clin Neurophysiol 17:377–396.

Demonet JF, Thierry G, Cardebat D (2005) Renewal of the neurophysiology of language: functional neuroimaging. Physiol Rev 85:49–95.

Edwards E, Soltani M, Deouell LY, Berger MS, Knight RT (2005) High gamma activity in response to deviant auditory stimuli recorded directly from human cortex. J Neurophysiol 94:4269–4280.

Edwards E, Soltani M, Kim W, Dalal SS, Nagarajan SS, Berger MS, Knight RT (2009) Comparison of time-frequency responses and the event-related potential to auditory speech stimuli in human cortex. J Neurophysiol 102:377–386.

Fries P, Nikolic D, Singer W (2007) The gamma cycle. Trends Neurosci 30:309–316.

Ghazanfar AA, Schroeder CE (2006) Is neocortex essentially multisensory? Trends Cogn Sci 10:278–285.

Herculano-Houzel S, Munk M, Neuenschwander S, Singer W (1999) Precisely synchronized oscillatory firing patterns require electroencephalographic activation. J Neurosci 19:3992.

Herrmann CS, Fründ I, Lenz D (2010) Human gamma-band activity: A review on cognitive and behavioral correlates and network models. Neurosci Biobehav Rev 34:981–992.

Hlawatsch F, Boudreaux-Bartels GF (1992) Linear and quadratic time-frequency signal representations. IEEE Signal Process Mag 9:21–67.

Indefrey P, Levelt WJ (2004) The spatial and temporal signatures of word production components. Cognition 92:101–144.

Jerbi K, Ossandón T, Hamamé C, Senova S, Dalal S, Jung J, Minotti L, Bertrand O, Berthoz A, Kahane P (2009) Task-related gamma-band dynamics from an intracerebral perspective: review and implications for surface EEG and MEG. Hum Brain Mapp 30:1758–1771.

Jobard G, Crivello F, Tzourio-Mazoyer N (2003) Evaluation of the dual route theory of reading: a metanalysis of 35 neuroimaging studies. Neuroimage 20:693–712.

Jones MS, MacDonald KD, Choi B, Dudek FE, Barth DS (2000) Intracellular correlates of fast (>200 Hz) electrical oscillations in rat somatosensory cortex. J Neurophysiol 84:1505–1518.

Kaiser J, Lutzenberger W (2003) Induced gamma-band activity and human brain function. Neuroscientist 9:475–484.

Kay SM, Marple SL Jr (1981) Spectrum analysis: a modern perspective. Proc IEEE 69:1380–1419.

Lancaster JL, Woldorff MG, Parsons LM, Liotti M, Freitas CS, Rainey L, Kochunov PV, Nickerson D, Mikiten SA, Fox PT (2000) Automated Talairach atlas labels for functional brain mapping. Hum Brain Mapp 10:120–131.

Mainy N, Jung J, Baciu M, Kahane P, Schoendorff B, Minotti L, Hoffmann D, Bertrand O, Lachaux JP (2008) Cortical dynamics of word recognition. Hum Brain Mapp 29:1215–1230.

Manning JR, Jacobs J, Fried I, Kahana MJ (2009) Broadband shifts in local field potential power spectra are correlated with single-neuron spiking in humans. J Neurosci 29:13613–13620.

Miller KJ (2010) Broadband spectral change: evidence for a macroscale correlate of population firing rate? J Neurosci 30:6477–6479.

Miller KJ, Makeig S, Hebb AO, Rao RP, denNijs M, Ojemann JG (2007) Cortical electrode localization from X-rays and simple mapping for electrocorticographic research: the "location on cortex" (LOC) package for MATLAB. J Neurosci Methods 162:303–308.

Miller KJ, Zanos S, Fetz EE, den Nijs M, Ojemann JG (2009) Decoupling the cortical power spectrum reveals real-time representation of individual finger movements in humans. J Neurosci 29:3132–3137.

Nunez PL, Srinivasan R (2006) Electric fields of the brain: the neurophysics of EEG, Ed 2. New York: Oxford UP.

Ojemann G, Ojemann J, Lettich E, Berger M (1989) Cortical language localization in left, dominant hemisphere. J Neurosurg 71:316–326.

Petersen S, Fiez J (1993) The processing of single words studied with positron emission tomography. Annu Rev Neurosci 16:509–530.

Ray S, Crone NE, Niebur E, Franaszczuk PJ, Hsiao SS (2008) Neural correlates of high-gamma oscillations (60–200 Hz) in macaque local field potentials and their potential implications in electrocorticography. J Neurosci 28:11526–11536.

Salmelin R (2007) Clinical neurophysiology of language: the MEG approach. Clin Neurophysiol 118:237–254.

Schalk G, McFarland DJ, Hinterberger T, Birbaumer N, Wolpaw JR (2004)

BCI2000: a general-purpose, brain-computer interface (BCI) system. IEEE Trans Biomedical Engineering 51:1034–1043.

Scott SK, McGettigan C, Eisner F (2009) A little more conversation, a little less action [mdash] candidate roles for the motor cortex in speech perception. Nat Rev Neurosci 10:295–302.

Sirota A, Montgomery S, Fujisawa S, Isomura Y, Zugaro M, Buzsáki G (2008) Entrainment of neocortical neurons and gamma oscillations by the hippocampal theta rhythm. Neuron 60:683–697.

Sukov W, Barth DS (1998) Three-dimensional analysis of spontaneous and thalamically evoked gamma oscillations in auditory cortex. J Neurophysiol 79:2875–2884.

Tallon-Baudry C (2009) The roles of gamma-band oscillatory synchrony in human visual cognition. Front Biosci 14:321–332.

Tallon-Baudry C, Bertrand O, Henaff MA, Isnard J, Fischer C (2005) Attention modulates gamma-band oscillations differently in the human lateral occipital cortex and fusiform gyrus. Cereb Cortex 15:654–662.

Towle VL, Yoon HA, Castelle M, Edgar JC, Biassou NM, Frim DM, Spire JP, Kohrman MH (2008) ECoG gamma activity during a language task: differentiating expressive and receptive speech areas. Brain 131:2013–2027.

Uhlhaas PJ, Pipa G, Lima B, Melloni L, Neuenschwander S, Nikolić D, Singer W (2009) Neural synchrony in cortical networks: history, concept and current status. Front Integr Neurosci 3:17:1–19.

Whittingstall K, Logothetis NK (2009) Frequency-band coupling in surface EEG reflects spiking activity in monkey visual cortex. Neuron 64:281–289.

Wyart V, Tallon-Baudry C (2008) Neural dissociation between visual awareness and spatial attention. J Neurosci 28:2667–2679.